Available online at www.sciencedirect.com
SCIENCE DIRECT®
Journal of Power Sources 132 (2004) 261–265
JOURNAL OF POWER SOURCES
www.elsevier.com/locate/jpowsour

Voltammetric and morphological study of lead electrodeposition on copper substrate for application of a lead–acid batteries

I.A. Carlos*, T.T. Matsuo, J.L.P. Siqueira, M.R.H. de Almeida

Departamento de Química, Universidade Federal de São Carlos, Caixa Postal 676, 13565-905 São Carlos, SP, Brazil

Received 11 December 2003; accepted 24 December 2003

Abstract

Electrodeposition of lead on copper was investigated experimentally, mainly the adherence of the lead plate and, if possible to obtain films with characteristics suitable for use in lead battery technology.

Under potentiodynamic and chronopotentiometric conditions, the lead films deposited from alkaline glycerol solutions on copper were sufficiently adherent for this substrate showed to be potentially useful as a cathode for lead deposition. Scanning electron microscopy (SEM) photographs showed that there was no dendritic growth of lead film on copper substrate, which is thus acceptable as a support in battery plates. With the help of energy dispersive X-ray spectroscopy (EDS), an explanation has been offered for the adherence of the lead deposits to the copper substrate. It was concluded that lead film deposited prior to lead bulk deposition favors the adhesion of the electrodeposits.

Keywords: Lead deposit; Copper substrate; Alkaline glycerol bath; Adherence; Recovery

1. Introduction

The study of the electrodeposition of lead on copper substrate is currently very relevant owing to its potential application in the Pb/H_2SO_4 battery area. Copper has been proposed as an alternative to lead alloys for grids in Pb/H_2SO_4 batteries [1,2], since the use of the copper supports in battery plates improves the conductivity of the grids. In order to use copper as the positive grids in Pb/H_2SO_4 batteries, it is required that the lead films be thick and adherent. This is necessary in view of due the danger of contamination of the battery electrolyte by copper due to corrosion during the life of the battery [1]. In previous studies [3], we have described the production of lead films on 1010 steel substrates using alkaline glycerol and alkaline sorbitol solutions. The lead deposits on 1010 steel were non-adherent and could be transformed into high-purity lead powder [3,4]. However, underpotential deposition of lead on copper [5–7] has been observed which could lead to bulk deposition with good adhesion. Extending our former studies, in this paper lead electrodeposition is reviewed with particular emphasis on the adherence of this film to a copper substrate. We examine whether the morphological characteristics of the lead films are acceptable and consistent with use as support in battery plates.

2. Experimental

All chemicals were analytical grade. Double-distilled water was used throughout. Each electrochemical experiment was performed in a non-cyanide bath containing 0.1 M $Pb(NO_3)_2 + 0.2$ M glycerol NaOH plus NaOH at various concentrations. A rotating Cu disk (0.283 cm^2), or a fixed plate (14.08 cm^2); a Pt plate and a Hg/HgO/1 M NaOH electrode with an appropriate Lugging capillary were employed as working, auxiliary and reference electrodes, respectively. The Cu substrate, from Aldrich, was 99.99% pure. Immediately prior to the electrochemical measurements, the Cu working electrodes were ground with emery paper, then rinsed with water. Potentiodynamic and chronopotentiometric measurements were recorded with a PAR model 173 potentiostat/galvanostat and a plotting recorder. All experiments were carried out at room temperature (25 °C). Scanning electron microscopy (SEM) micrographs were taken with a Carl Zeiss Microscope, Model DMS 940A, connected to an X-ray microanalysis system, Model AN10/55S, for energy dispersive X-ray spectroscopy (EDS) measurements.

* Corresponding author. Tel.: +55-16-260-8208; fax: +55-16-260-8350.
E-mail address: ivani@dq.ufscar.br (I.A. Carlos).

0378-7753/$ – see front matter © 2004 Elsevier B.V. All rights reserved.
doi:10.1016/j.jpowsour.2003.12.047

3. Results and discussion

3.1. Electrodeposition of Pb on copper substrate

Fig. 1 shows voltammograms for the stationary copper substrate in the Pb plating bath at various NaOH concentrations and in the solutions 0.6 and 2.0 M NaOH (Fig. 1a and b) all in the presence of 0.2 M glycerol. In Fig. 1, two cathodic peaks, c_1 and c_2, can be seen and the deposition process, in the region of peak c_2, is strongly reversible and exhibits a high charge current density (i_0). The peak c_1 can be attributed to lead film deposition and/or copper oxide reduction and peak c_2 to lead bulk deposition. Also, it can be verified in this figure that the presence of different NaOH concentrations does not shift the deposition potentials, whereas for Pb deposition on 1010 steel, such a shift was observed [3].

The H_2 evolution overpotential on the copper disk electrode was studied in the absence of the plating salts. Fig. 1a and b shows the cathodic voltammograms for this substrate in 0.6 and 2.0 M NaOH, in the presence of 0.2 M glycerol. It can be seen that H_2 evolution does not affect the voltammetric deposition of Pb in the initial moments of the plating process. It is only really significant at potentials beyond −1.4 V. Also, two cathodic peaks can be observed in the cathodic scan, which correspond to copper oxide reduction [8–10].

In order to analyze the process occurring in the region of peak c_1 (Fig. 1), the cathodic and anodic behavior of the copper electrode in 0.6 M NaOH and 0.2 M glycerol without Pb^{2+} ions was studied, as shown in Fig. 2a (solid line). For comparison, the voltammogram of the copper electrode

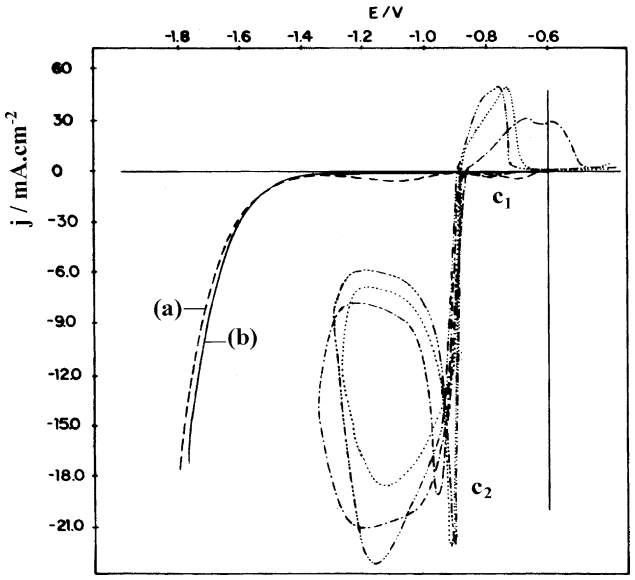

Fig. 1. Voltammetric curves for copper substrate in 0.1 M $Pb(NO_3)_2$ + 0.2 M glycerol at various NaOH concentrations: (–·–) 0.6 M NaOH, (···) 1.5 M NaOH, (–···–) 2.0 M NaOH, at 10 mV s^{-1}. Voltammetric curves for copper in: 0.2 M glycerol and (a) 0.6 M NaOH, (b) 2.0 M NaOH, at 10 mV s^{-1}.

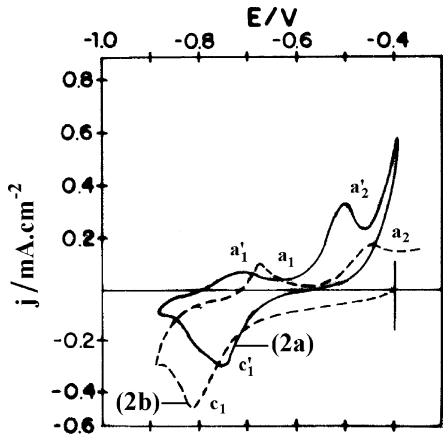

Fig. 2. Voltammetric curves for copper substrate in: (a) 0.2 M glycerol + 0.6 M NaOH, (b) 0.1 M $Pb(NO_3)_2$ + 0.2 M glycerol + 0.6 M NaOH, at 10 mV s^{-1}.

in 0.1 M Pb^{2+}, 0.6 M NaOH and 0.2 M glycerol is given in Fig. 2b (dashed line). Fig. 2a shows a peak c'_1 (q_d = 4.1 mC cm^{-2}) at −0.750 V in the cathodic forward scan, which can be attributed to the reduction of copper oxide formed at the start of the scan, because the return sweep shows peaks a'_1 (−0.730 V) and a'_2 (−0.510 V) in this potential range. Fig. 2b represents the voltammogram for lead

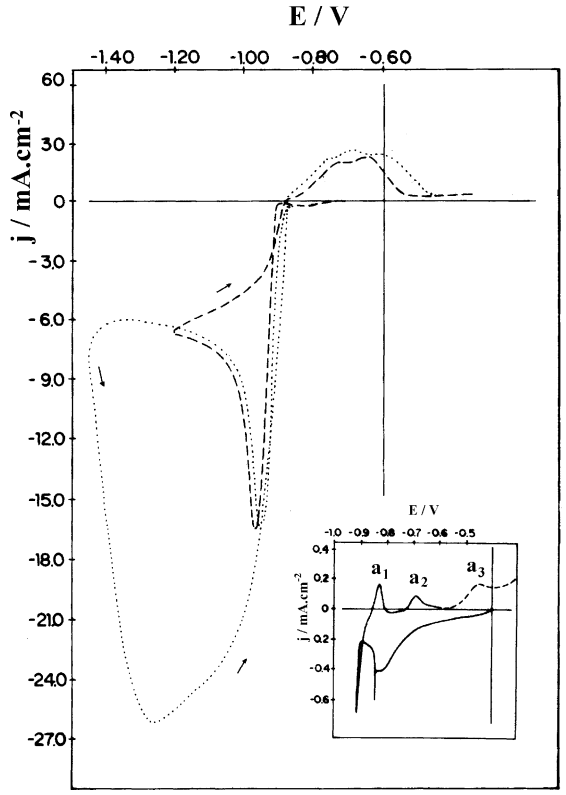

Fig. 3. Voltammetric curves for copper substrates in: 0.1 M $Pb(NO_3)_2$ + 0.2 M glycerol + 0.6 M NaOH and effect of the cathodic potential limit values: −1.20 V (– – –), −1.44 V (···) and −0.94 V (inset), at 10 mV s^{-1}.

deposition on copper, and shows a peak c_1 in the cathodic part. The charge density of peak c_1 ($q_d = 7.3\,mC\,cm^{-2}$) is larger than that of peak c_1' ($q_d = 4.1\,mC\,cm^{-2}$), suggesting that some reduction of Pb^{2+} species might be occurring together with the copper oxide reduction. In the literature, similar behavior has been observed when copper was deposited simultaneously with iron oxide reduction [4]. Also in Fig. 2b, two anodic peaks, a_1 (−0.680 V) and a_2 (−0.460 V) can be seen, in the return scan, which correspond to copper oxide formation, since their potentials are in the same range as copper oxide (Fig. 2a). Although no anodic lead dissolution peak is visible in this region of potential, the presence of lead crystallites was confirmed by EDS, as discussed further on. Thus, it can be suggested that lead bulk deposition, in the region of peak c_2 (Fig. 1), occurs on the new sites on the copper substrate formed by reduction of copper oxides and on the lead film deposited in the region of peak c_1. Underpotential deposition (UPD) of lead on copper has been observed previously [4–6]. However, the value of the charge density of peak c_1 is $7.3\,mC\,cm^{-2}$, which cannot be attributed to lead UPD.

These results imply that the adherence of the lead electrodeposits on copper substrate (reported late in this section) is probably due to the process that occurs in the region of peak c_1, which was not observed during lead deposition on 1010 steel substrate [3].

Fig. 3 shows stationary cyclic voltammograms with different lower-limit potentials. When the sweep is reversed at potential −0.91 V (insert in Fig. 3) a crossover can be seen, which suggests nucleated electrodeposition in this region [11,12]. After the lead deposition, the cathodic current decreases fast before the formation of three anodic peaks a_1, a_2 and a_3, in the returned scan peak a_1 corresponds to bulk Pb dissolution and peaks a_2 and a_3 to copper oxide formation, since their potentials are in the same potential range as copper oxide (peaks a_1' and a_2', Fig. 2a). When the sweep is reversed at potential −1.20 V (Fig. 3, dashed line), the current decreases, indicating that the plating process is under mass-transport control. Finally, at a limit potential of −1.44 V (Fig. 3, dotted line), in the reverse scan the cathodic current increases, indicating a large increase in the area of deposition due to a second nucleation process.

Fig. 4 illustrates the effect of the potential scan rate (υ) on peaks c_1 and c_2. It can be seen that the current densities in

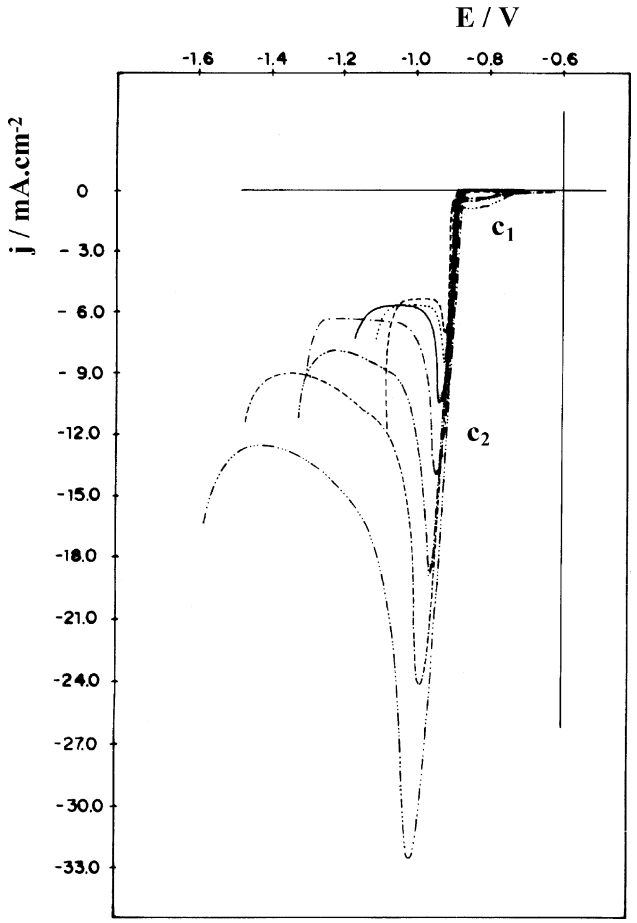

Fig. 4. Voltammetric curves for copper substrates in 0.10 M $Pb(NO_3)_2$ + 0.2 M glycerol + 0.6 M NaOH, at various sweep rates (υ, $mV\,s^{-1}$): 0.5 (–/–), (—) 1.0; (– – –) 2.0; (- - -) 5.0; (–·–) 10; (–··–) 20; (–····–) 50.

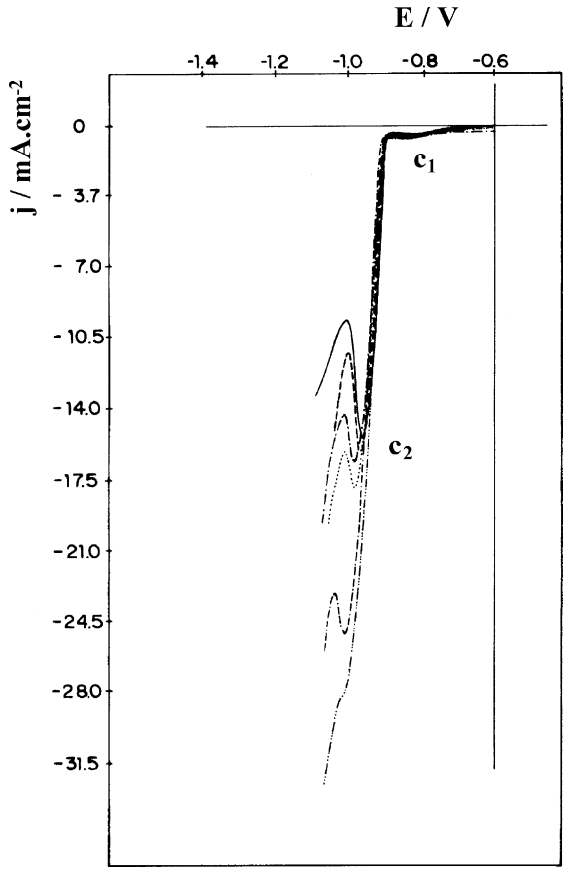

Fig. 5. Voltammetric curves for copper substrates in 0.10 M $Pb(NO_3)_2$ + 0.20 M glycerol + 0.6 M NaOH at various rotation speeds (ω, Hz): (—) 0.21; (– – –) 0.46; (- - -) 1.0; (–·–) 1.25; (–··–) 1.5; (–····–) 1.72, at $10\,mV\,s^{-1}$.

the region of peak c_2 depend strongly on potential scan rate, while the dependence is insignificant in the region of peak c_1. These data suggest that the lead bulk reduction process (peak c_2) is largely mass-transport controlled.

To confirm these results obtained with the stationary electrode concerning the mass-transport control of the deposition process, studies with a rotating disk electrode (RDE) were made [13]. Fig. 5 displays the voltammetric curves for the RDE at various rotation speeds (ω). These results show that in the initial moments of the deposition process there is no contribution from mass-transport control, as the deposition current densities are independent of the rotation speeds. Only at the peak c_2 does mass-transport become important. Compared with Fig. 1, the current densities on the rotating disk electrode are much higher, indicating that the limiting current densities observed on the stationary electrode are due to mass-transport limitation.

The lead electrodeposits were obtained chronopotentiometrically on copper plate substrates, in a range of cathodic current densities of 1.8–24.7 mA cm^{-2}, and tested for adherence in accordance with standard methods in ASTM D

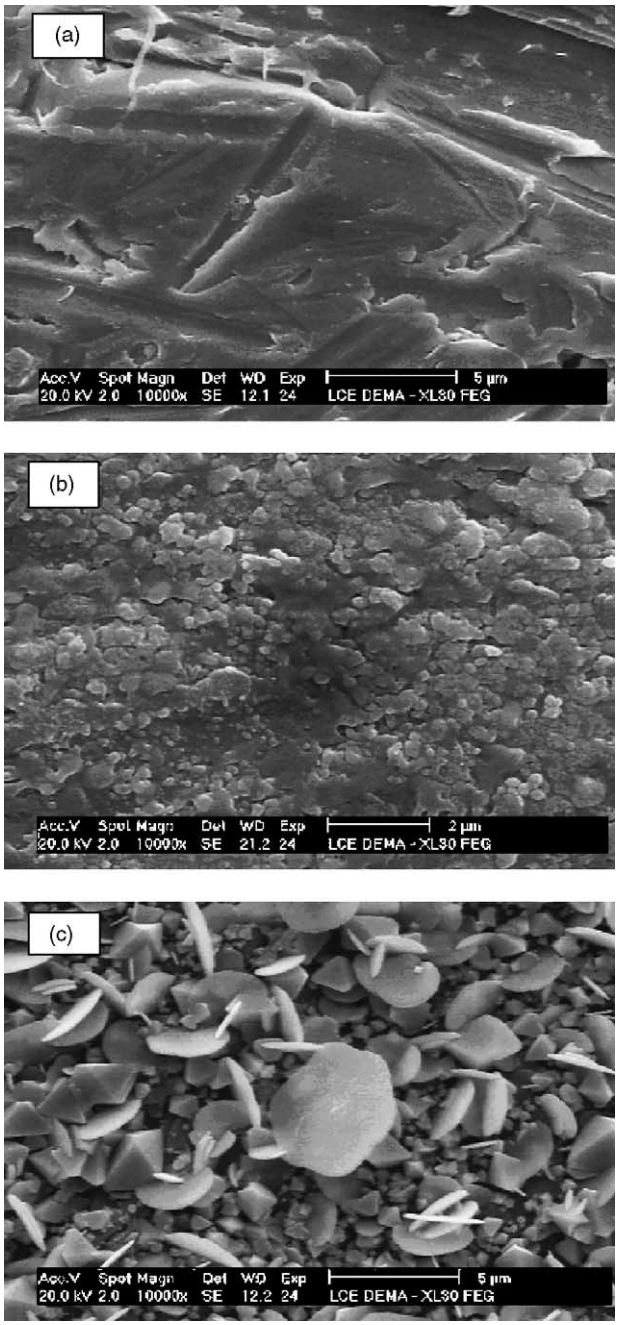

Fig. 6. SEM micrographs for lead films obtained from −0.60 V to various potentials as in Fig. 1: (a) −0.89 V; (b) −0.95 V; (c) −1.25 V. Electrolytic solution: 0.10 M $Pb(NO_3)_2$ + 0.20 M glycerol + 0.6 M NaOH.

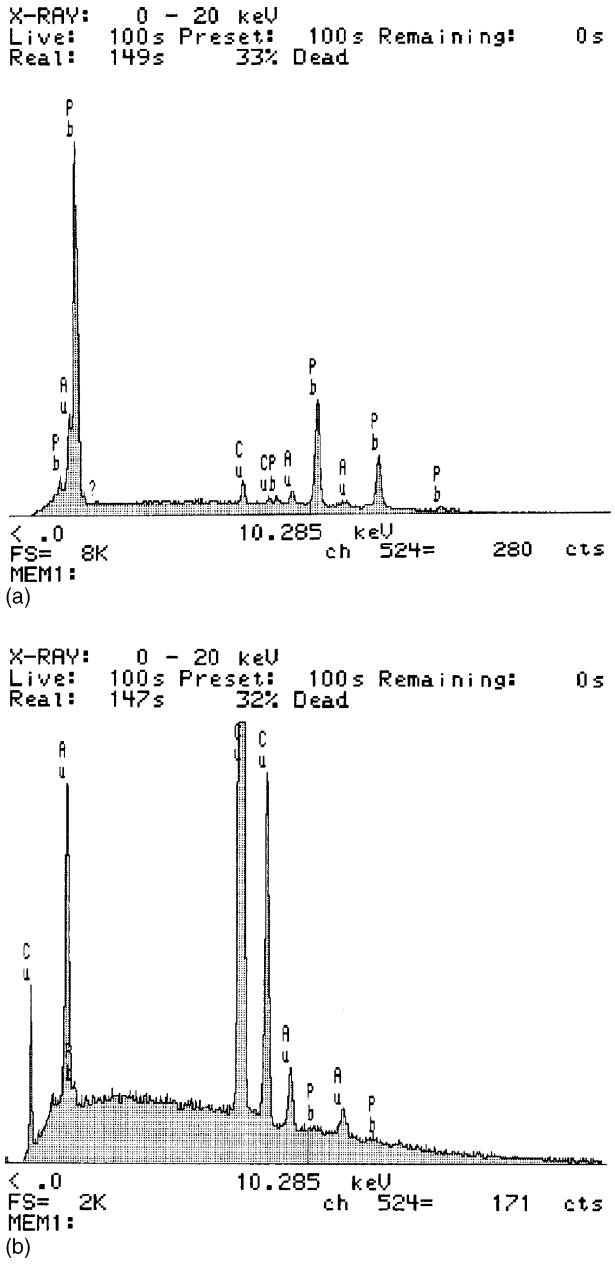

Fig. 7. EDS analysis of Pb films on copper substrate obtained chronoamperometrically (a) from −0.60 to −0.80 V, q_d = 2.5 C cm^{-2} and potentiodynamically (b) from −0.60 at −0.80 V. Electrolytic solution: 0.10 M $Pb(NO_3)_2$ + 0.20 M glycerol + 0.6 M NaOH.

3359 [14]. According to this norm, the lead deposits were classified as No. 5, indicating that the films were strongly adherent. It can be concluded that these lead films on copper substrates can be used as the support in battery plates.

3.2. Morphology of lead electrodeposits

In the potential range from −0.60 to −0.89 V (Fig. 1), the substrate is covered in homogeneous lead film (Fig. 6a). During the scan from −0.30 to −0.95 V (top peak c_2, Fig. 1) completely coalesced lead globular crystallites were observed (Fig. 6b). After the scan from −0.30 to −1.25 V (Fig. 1), a lead film was observed with various geometric forms, such as pyramids, plates and globules, which totally covered the copper substrate (Fig. 6c). These results are significant in showing there is no propagation of dendrite growth when the potentials are more negative than −0.95 V. Also, they corroborate those obtained for lead on 1010 steel [3].

EDS showed the presence of lead film on the Cu substrate, obtained chronoamperometrically from −0.60 to −0.80 V at a charge density of 2.5 C cm^{-2} (Fig. 7a). Also, for comparison, Fig. 7b shows EDS of lead film on Cu substrate obtained potentiodynamically from −0.60 at −0.80 V (region of peak c_1). These results show that lead film is already deposited in the initial moments of deposition process, corroborated the data shown in Fig. 2a. It can be inferred that formation of lead film and reduction of copper oxide are possible in the region of peak c_1.

4. Conclusions

Potentiodynamic curves indicated that the lead deposition process is characterized by two peaks, c_1 and c_2 (film and bulk deposition, respectively). The lead deposition rate is high in the region of peak c_2 and controlled by a mass-transport limit beyond this peak. The peak c_1 corresponds to two simultaneous electrochemical reactions: Pb(II) ion and copper oxide reduction. The lead film on copper substrate was strongly adherent and thus can be used as support in battery plates. From the SEM results it can be seen that there are no propagation of dendrites, even at very negative deposition potentials. EDS showed the presence of lead film on the Cu substrate from the initial moments of the deposition process.

References

[1] N.E. Bagshaw, J. Power Sources 53 (1995) 23–30.
[2] L.A. Yolshina, V.Ya. Kudyakov, V.G. Zyryanov, J. Power Sources 65 (1997) 71–76.
[3] I.A. Carlos, M.A. Malaquias, M.M. Oizume, T.T. Matsuo, J. Power Sources 92 (2001) 56–64.
[4] I.A. Carlos, J.L.P. Siquiera, G.A. Finazzi, M.R.H. de Almeida, J. Power Sources 117 (2003) 179–186.
[5] L. Bonou, M. Eyraud, J. Crousier, J. Appl. Electrochem. 24 (1994) 906–910.
[6] J. Horkans, I.H. Chang, H. Deligianni, P.C. Andricacos, J. Electrochem. Soc. 142 (7) (1995) 2244–2249.
[7] Y.S. Chu, I.K. Robison, A.A. Gewirth, Phys. Rev. 55 (12) (1997) 7945–7954.
[8] M.R.H. de Almeida, I.A. Carlos, L.L. Barbosa, R.M. Carlos, B.S. Lima-Neto, E.M.J.A. Pallone, J. Appl. Electrochem. 32 (2002) 763–773.
[9] M.A.C. Berton, Ph.D. thesis, Universidade Federal de São Carlos, Brasil, 1994.
[10] L.L. Barbosa, Ph.D. thesis, Universidade Federal de São Carlos, Brasil, 2000.
[11] G. Gunawardena, G. Hills, I. Montenegro, B. Sharifker, J. Electroanal. Chem. 138 (1982) 225–239.
[12] S. Fletcher, Electrochim. Acta 28 (7) (1983) 917–923.
[13] B.J. Allen, L. Faulkner, Electrochemical Methods. Fundamentals and Applications, John Wiley & Sons, New York, 1980.
[14] American Society for Testing and Materials, Standard Methods for Measuring Adhesion by Tape Test, D 3359-78, Philadelphia, vol. 27, 1979, pp. 704–708.